Validation of Cartilage Thickness Calculations Using Indentation Analysis

Matthew F. Koff[1]
Assistant Scientist
Department of Radiology and Imaging,
Hospital for Special Surgery,
New York, NY 10021
e-mail: koffm@hss.edu

Le Roy Chong
Department of Diagnostic Radiology,
Changi General Hospital,
Singapore 529889, Singapore

Patrick Virtue
GE Healthcare,
Waukesha, WI 53188

Dan Chen

Xioanan Wang

Timothy Wright

Department of Biomechanics,
Hospital for Special Surgery,
New York, NY 10021

Hollis G. Potter
Department of Radiology and Imaging,
Hospital for Special Surgery,
New York, NY 10021

Different methods have been used to cross-validate cartilage thickness measurements from magnetic resonance images (MRIs); however, a majority of these methods rely on interpolated data points, regional mean and/or maximal thickness, or surface mean thickness for data analysis. Furthermore, the accuracy of MRI cartilage thickness measurements from commercially available software packages has not necessarily been validated and may lead to an under- or overestimation of cartilage thickness. The goal of this study was to perform a matching point-to-point validation of indirect cartilage thickness calculations using a magnetic resonance (MR) image data set with direct cartilage thickness measurements using biomechanical indentation testing at the same anatomical locations. Seven bovine distal femoral condyles were prepared and a novel phantom filled with dilute gadolinium solution was rigidly attached to each specimen. High resolution MR images were acquired, and thickness indentation analysis of the cartilage was performed immediately after scanning. Segmentation of the MR data and cartilage thickness calculation was performed using semi-automated software. Registration of MR and indentation data was performed using the fluid filled phantom. The inter- and intra-examiner differences of the measurements were also determined. A total of 105 paired MRI-indentation thickness data points were analyzed, and a significant correlation between them was found ($r=0.88$, $p<0.0001$). The mean difference ($\pm$std. dev.) between measurement techniques was 0.00 ± 0.23 mm, with Bland–Altman limits of agreement of 0.45 mm and -0.46 mm. The intra- and inter-examiner measurement differences were 0.03 ± 0.22 mm and 0.05 ± 0.24 mm, respectively. This study validated cartilage thickness measurements from MR images with thickness measurements from indentation by using a novel phantom to register the image-based and laboratory-based data sets. The accuracy of the measurements was comparable to previous cartilage thickness validation studies in literature. The results of this study will aid in validating a tool for clinical evaluation of in-vivo cartilage thickness. [DOI: 10.1115/1.4000989]

Keywords: MRI, cartilage, imaging, measurement

1 Introduction

Due to its lack of ionizing radiation and superior soft tissue contrast, magnetic resonance imaging (MRI) is an effective tool for visualizing articular cartilage [1], particularly in the setting of osteoarthritis (OA). OA affects over 20 million adults in the United States and is the leading cause of disability [2]. Changes in articular cartilage due to OA include fibrillation of the articular surface, increased permeability, reduced proteoglycan content, and a shift of joint load to the solid component of the tissue [3], which leads to further depletion of matrix and loss of cartilage thickness. Morphologic MR images of articular cartilage are commonly acquired to determine pathologic changes in the tissue and are an effective tool for evaluating OA and the localization of chondral lesions [4]. Advanced quantitative MRI techniques such as T2 mapping and T1ρ mapping [5,6] and delayed gadolinium enhanced MRI of cartilage (dGEMRIC) [7,8] highlight subtle biochemical changes within articular cartilage during the early onset of OA. However, many investigators have used cartilage thickness and volume measurements as a method to track cartilage degeneration [9].

Specific MRI acquisition techniques produce images optimal for volumetric and thickness analysis of articular cartilage [1]. Images for quantitative cartilage morphologic analysis are commonly constructed using a three-dimensional (3D) image acquisition method (e.g., 3D-spoiled gradient recalled (SPGR) [10–12], 3D-fast low angle shot (FLASH) [13,14], or 3D-double echo steady state (DESS) [15,16]). Measurements and other quantities calculated from the generated MR images must be validated to ensure an accurate representation of the quantity being measured, independent of specific imaging protocol.

Several studies used different methods to cross-validate cartilage thickness measurements from MR images, including stereophotogrammetry [17], acquiring anatomical sections [14,18–23], faxitron X-ray [11], computed tomography arthrography [12,24–27], ultrasound [13,25,28,29], or laser scanning [10,30]. A majority of these methods rely on interpolated data points, regional mean and/or maximal thickness, or surface mean thickness for data analysis. Using averaged data sets for thickness validation may artificially increase the accuracy of the measurements since the effect of any local cartilage thickness measurement is minimized. Most studies did not include the ability to accurately perform an accurate matching "point-to-point" criterion for statistical comparison. Furthermore, the accuracy of MRI cartilage thickness measurements from commercially available software packages has not necessarily been validated and may lead to an under- or overestimation of cartilage thickness. Validation of indirect cartilage thickness measurements from a MR image data set is strengthened by direct measurements at the same anatomical locations.

[1]Corresponding author.

Contributed by the Bioengineering Division of ASME for publication in the JOURNAL OF BIOMECHANICAL ENGINEERING. Manuscript received November 12, 2009; final manuscript received January 11, 2010; accepted manuscript posted January 12, 2010; published online March 18, 2010. Editor: Michael Sacks.

Our goal was to perform a matching point-to-point validation of indirect cartilage thickness calculations using a 3D-SPGR MRI data set with direct cartilage thickness measurements using biomechanical indentation testing at the same anatomical locations. The focus of validating cartilage thickness measurements and not cartilage volume is due to our clinical environment, which emphasizes the need for accurate assessment of local cartilage degeneration when planning for surgical intervention. Furthermore, a global measure of cartilage volume does not identify specific locations where cartilage degeneration may be occurring. The approach required registering two independent data sets by using a phantom that was easily located in both data acquisition coordinate systems. Based on previous investigations [18,25], we set a threshold value of 0.5 mm for successful matching of our thicknesses as measured from these two techniques.

2 Methods and Materials

2.1 Specimen Preparation. Seven adult bovine stifle (knee) joints were acquired from a local abattoir. The knees were stripped of all soft tissues and were carefully disarticulated to prevent damage to the articular cartilage of the distal femur. The femur was cut in half sagittally to separate the condyles. The femoral cartilage was kept hydrated with physiologic saline solution during the entire preparation process. An L-shaped phantom, composed of polycarbonate, was rigidly attached to each condyle using nylon screws at a position close to the articular surface (Fig. 1). The phantom was 5 mm thick with arm lengths of 20 mm and was manufactured to an accuracy of 25 μm in each dimension. The arms of the phantom were hollow and filled with a dilute gadolinium solution (1:200 v/v). The condyle was then submerged in a container of vegetable oil prior to MR scanning. A material containing sodium polyacrylate was saturated with water and wrapped around the specimen container to increase the regional signal intensity. The combination of submersing the specimen in oil with chemical selective fat-suppression scanning ensured a clear delineation of the articular surface and minimized noise [11], as determined from pilot scans.

2.2 Data Acquisition. All scanning was performed on a 3.0 T clinical MRI system (GE Healthcare, Waukesha, WI) with an eight-channel phased array knee coil. A 3D T1 weighted fat-suppressed SPGR echo image data set was acquired for cartilage segmentation and thickness quantification (repetition time (TR): 13.2 ms, echo time (TE): 2.7 ms, field of view (FOV): 13 cm, flip angle: 10 deg, slice thickness: 0.7 mm, matrix: 512×512, receiver bandwidth: ± 62.5 kHz, and number of excitations (NEX): 3). The resulting in-plane resolution was 0.25×0.25 mm^2. Scanning required about 25 min for each specimen.

Needle indentation testing of the cartilage was performed immediately following imaging (Fig. 2). The proximal end of the femur was secured in a custom positioning device and was mounted to an EnduraTEC material testing system (ELF 3200, Bose Corp., Eden Prairie, MN). The articular surface of the distal femur was oriented perpendicular visually by an experienced technician to an indentation needle ($\varnothing = 0.6$ mm, length $= 7$ mm). The needle was attached to a load cell (1000 g, Honeywell-Sensotec, Model 31), which was attached to the EnduraTEC system. A 3D digitizing stylus with a needle-tipped probe (Microscribe G2x, Immersion Corp, San Jose, CA) (accuracy: 0.23 mm) was used to determine the site of indentation testing relative to a laboratory coordinate system (LCS) defined by points etched on the surface of the phantom. Cartilage indentation was performed at a constant displacement rate of 0.05 mm/s. A small increase in measured force denoted initial contact with the cartilage surface, followed by a rapid increase in force when contact with underlying bone, occurred. The differences in displacement between the two phenomena denoted the cartilage thickness (Fig. 2). The technician used a custom written MATLAB (Mathworks, Natick, MA) program to aid in determining the cartilage thickness based on the change in measured tissue stiffness [31].

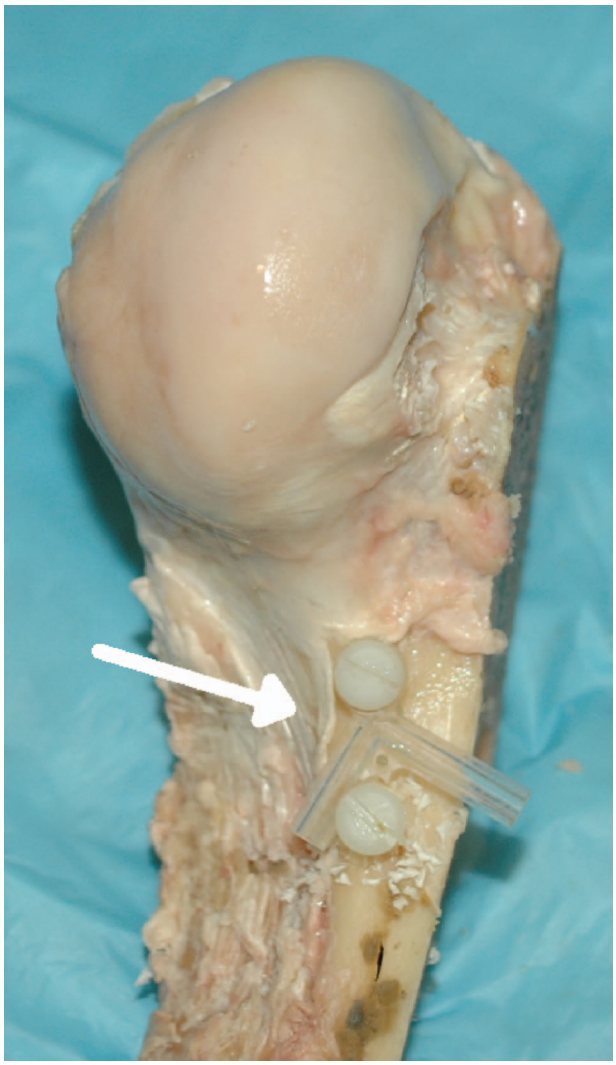

Fig. 1 Prepared bovine femoral condyle with L-phantom rigidly attached (arrow) using nylon screws

The accuracy of the indentation system was previously determined to be 2–5% of the actual thickness being measured, comparable to other methods of thickness measurement [30]. The point of indentation was marked with ink to ensure sufficient spacing between collected data points. Indentation testing was repeated for points across the articular surface, which were within the working volume of the indentation device. Indentation points were localized to the central portion of the condyle, in an effort to minimize errors due to out-of-plane curvature of the articular surface. The indented points were separated by about 6 mm. Approximately 18 points were acquired for each femoral condyle examined.

2.3 Data Analysis. The MR image data were analyzed using custom written semi-automated software (GE Healthcare, Waukesha, WI). First, the hyperintense voxels of the gadolinium solution within the phantom were identified and segmented within the MR coordinate system (MRCS) (Fig. 3). The location of the phantom in the MRCS was determined by fitting a digital solid model of the phantom to the hyperintense voxels of the gadolinium solution segmented from the MR data. The solid model was created from the known dimensions of the manufactured phantom. The custom software allowed the user to adjust the rigid registration manually

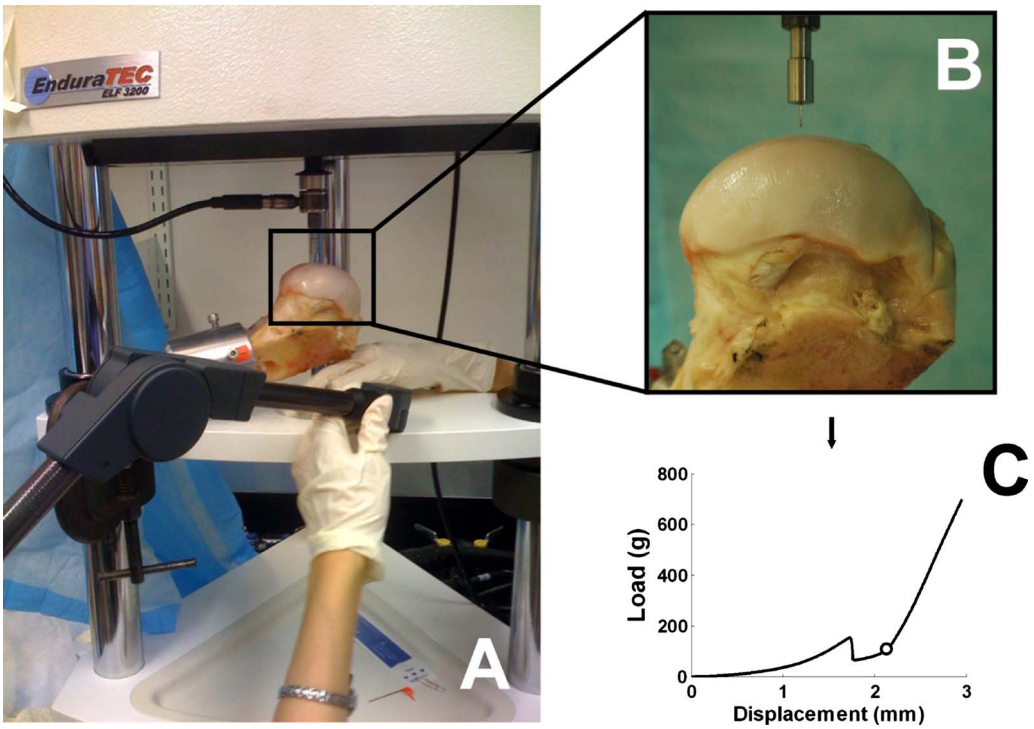

Fig. 2 Needle indentation testing to measure cartilage thickness. (*a*) Specimen mounted in the material testing system for indentation testing. A 3D digitizing stylus was used to record phantom location and orientation and site of indentation in the LCS. (*b*) Close-up of indentation test using needle probe oriented perpendicular to the articular surface. (*c*) Representative force-displacement curve from indentation at one testing location. The circle indicates cartilage thickness.

between the digital phantom and the segmented phantom until the fit accuracy was greatest. The software determined a fit accuracy value by calculating how many of 880 predetermined points within the digital phantom fell within the segmented hyperintense voxels.

Next, the cartilage of the condyle was manually segmented, and the deep and superficial surfaces of the cartilage were defined. The fat-saturation pulse sequence used displayed the cartilage as hyperintense voxels and the bone with little to no signal intensity (Fig. 3). An iterative closest point calculation method was used to define cartilage thickness. Finally, the locations from the indentation testing were transformed to the MRCS by aligning the coordinates of the phantom in the LCS with coordinates of the phantom in the MRCS. This alignment enabled a one-to-one pairing of cartilage thickness calculations/measurements between the LCS and MRCS.

2.4 Repeatability Analysis. Two examiners segmented, registered, and analyzed each bovine data set two times. The different data analysis sessions were separated by more than 24 h. All data processing and analysis by the two individuals was performed separately from one another. One examiner had extensive experience of performing the segmentation and data set transformations and the second examiner was newly introduced to segmenting data sets and data processing. Training data sets for the repeatability analysis were provided to both examiners from pilot scans.

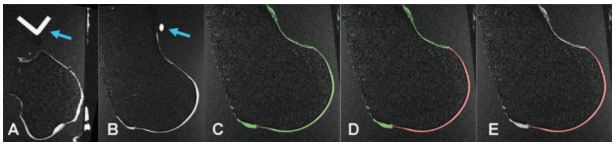

Fig. 3 ((*a*) and (*b*)) Reformatted images used to display, localize, and define the location of the L-phantom (arrows) in the MR coordinate system. Image slice showing user set threshold (*c*), semi-automated segmentation (*d*), and final segmentation (*e*) of the femoral condyle.

2.5 Statistical Analysis. A regression and correlation analysis was performed between the MR thickness and the indentation thickness data. Bland–Altman analysis between the two data sets was also performed since correlation does not account for systematic errors of each measurement system [32]. The Bland–Altman plot displays the average thickness of a point calculated by MRI and indentation on the ordinate and the difference of the measurements on the abscissa. The limits of agreement were calculated as the average thickness difference $\pm 2 \cdot$std. dev. of thickness differences and represent the range over which 95% of the differences are expected to occur [32]. Deviations of measurements were reported as systematic (comparison of pairwise differences including $\pm$ offsets) and absolute or random deviations (comparison of pairwise differences not including $\pm$ offsets) [13]. Inter- and intra-examiner repeatabilities of cartilage thickness calculations were calculated using the Bland–Altman calculation of 1.96 std. dev. of the average thickness difference [32], as well as calculation of the root mean square error (RMSE) and coefficient of variation (COV) of the thicknesses, as outlined previously by Glüer et al. [33].

3 Results

A total of 105 paired MRI-indentation thickness data points were analyzed from the 7 bovine condyles. The Pearson correlation coefficient (r) between the variables was significant ($r = 0.88$, $p < 0.0001$) (Fig. 4). The Bland–Altman analysis found cartilage thickness differences of 0.00 ± 0.23 mm (mean $\pm$ std. dev.) between the MRI analysis and indentation measurement (Fig. 5). The upper and lower limits of agreement were 0.45 mm and -0.46 mm, respectively. The systematic deviations were $0.9 \pm 19.0\%$, and the absolute deviations were $13.7 \pm 13.2\%$. The

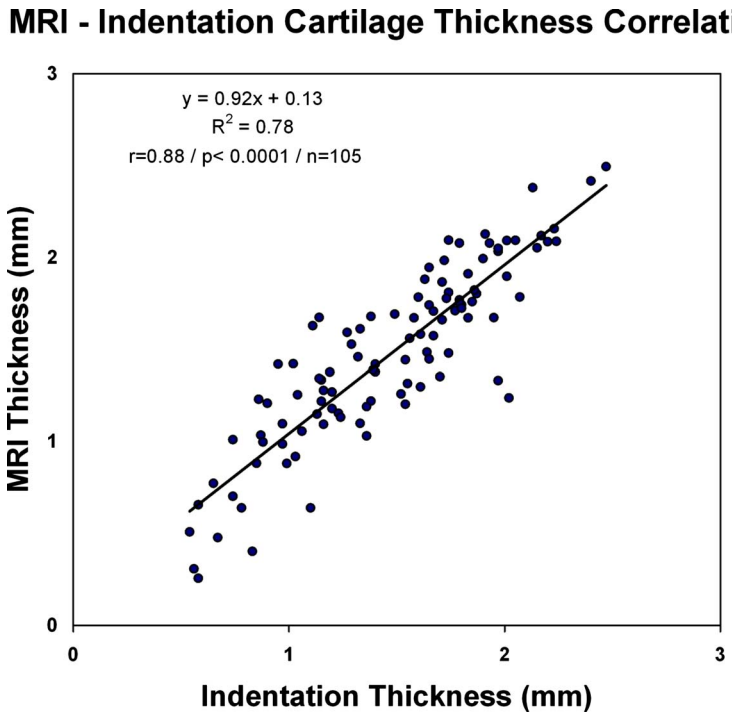

Fig. 4 Correlation plot of MR thickness measurements versus indentation thickness measurements. A significant correlation between the paired measurements was found.

intra-examiner thickness differences were 0.03 ± 0.22 mm, with a repeatability of 0.43 mm, a RMSE of 0.15 mm, and a COV of 10.2%. The inter-examiner thickness differences were 0.05 ± 0.24 mm, with a repeatability of 0.47 mm, a RMSE of 0.17 mm, and a COV of 11.3%.

4 Discussion

We validated cartilage thickness measurements on a point-by-point basis between a MR imaging and indentation data sets. Good correlation and minimal differences were found between the

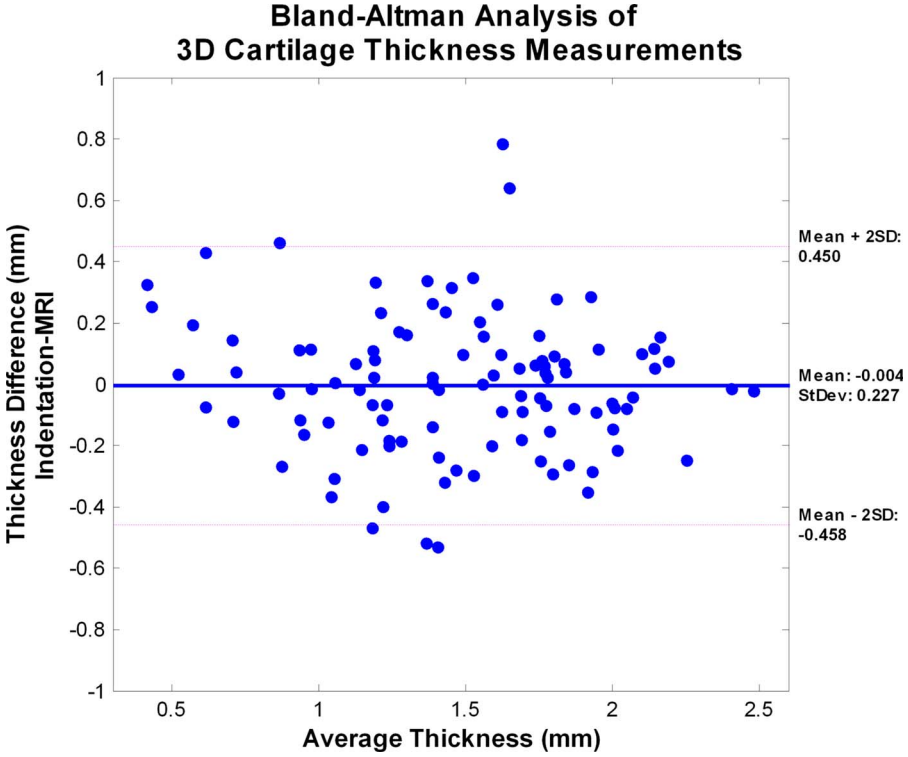

Fig. 5 Bland–Altman analysis of paired MR and indentation thickness measurements displaying mean difference (solid line) and limits of agreement (dashed lines)

measurement techniques. Combining the separate data sets was possible by using a novel MR phantom that was manufactured to high precision.

The accuracy of our cartilage thickness measurements is comparable to previous cartilage thickness validation studies in literature. The correlation found in this study is similar to a previous report of MR and cartilage thickness measurements from anatomical sections [20], which reported Pearson correlations of $r = 0.69-0.88$. A study by Yeh et al. [23] used specific anatomic landmarks to perform a matching point-to-point analysis of proximal humeral and glenoid cartilage thicknesses measured with MR arthrography and direct anatomic section analysis. Correlation coefficients of 0.73–0.87 were reported. We reprocessed the data presented by Yeh et al. [23] to perform a Bland–Altman analysis. Our reanalysis of their data found mean differences of 0.25 ± 0.55 mm for the humeral head and -0.17 ± 0.51 mm for the glenoid fossa, indicating limits of agreement of approximately 1.35 mm and -0.85 mm, and 0.85 mm and -1.19 mm for each bone, respectively. These limits of agreement are about twice those of the current study. A Bland–Altman analysis was also performed using the mean tibial and patellar cartilage thickness data reported by Graichen et al. [14], with correlations of $r = 0.72-0.97$ and absolute cartilage thickness differences of 4.3–12.3%. Our reanalysis produced a mean difference of 0.02 ± 0.13 mm, and limits of agreement of 0.28 mm and -0.24 mm, which are closer to our study. We also reanalyzed the tibial and talar dome cartilage data presented by El-Khoury et al. [12] and found a mean difference of 0.10 ± 0.21 mm and limits of agreement of 0.53 mm and -0.32 mm. The range of cartilage thickness differences found in previous studies may be attributed to the different in-plane and out-of-plane resolutions of the image sets, the potential of decreased signal-to-noise ratio (SNR) due to decreased magnetic field strengths, the anatomy scanned, and the method used to validate the MR measurements. The studies by Graichen et al. [14] and El-Khoury et al. [12] used anatomy with cartilage thickness similar to the current study. Finally, previous studies have reported that 61.1–84.5% of measurements were within 0.5 mm of the actual value [18], with lower estimates of 50% of measurements [25]. For the 105 paired measurements evaluated in this study, 96% of the matched data points were within 0.5 mm of each other.

The inter- and intra-examiner repeatabilities of the cartilage thickness measurements are also comparable to previous reports in literature. Karvonen et al. [21] reported intra- and inter-observer COVs of 3.2–10.5% and 12.8–23.2%, respectively. Muensterer et al. [22] reported a cartilage thickness COV of 3–6% using surface wide average cartilage thickness values. Kladny et al. [20] used mean cartilage thickness to achieve intra- and inter-observer differences of 0.39 ± 0.31 mm and 0.39 ± 0.33 mm, respectively. The elevated COV values of our study are likely due to the point-by-point nature of the analysis. Using a regional or overall surface average cartilage thickness for statistical analysis reduces any spurious local errors associated with a measurement technique.

An advantage of our study was the use of a registration novel phantom to compare cartilage thickness measurements from MRI data with indentation analysis on a point-by-point basis. The registration allowed for comparison of indirect MRI cartilage thickness calculations with direct indentation cartilage thickness measurements at the same anatomical location. The accuracy of the registration was determined from the overlap of the segmented voxels of the contrast fluid within the phantom with a geometric solid model of the phantom in the analysis software. The overlap of the two volumes consistently covered over 97% of the segmented contrast agent voxels for both examiners.

Our novel experimental method combined two distinct data sets: voxels representative of the contrast agent in the phantom and surface coordinates of the phantom from a digitizing probe. The common framework between the data sets is the known dimensions of the phantom, accurate to 25 μm, which were used for the data registration. Registering the two testing coordinate systems, MR- and laboratory-based, allowed for a point-by-point comparison of cartilage thickness. The one-to-one analysis is beneficial over reporting cartilage thickness measurements using interpolated [11], regional mean thickness [10,19], or overall articular surface mean thickness [14] because the data are site specific. Furthermore, the 3D indentation measurements and 3D cartilage thickness calculations allowed for out-of-plane curvature of the articular surface, which may affect validation of cartilage thickness measurements [11,24].

Our study had several limitations. The anatomy evaluated was that of the distal bovine femoral condyles and not human femoral condyles. The mean cartilage thickness measured was approximately 1.5 mm, slightly thinner than the reported range of articular cartilage thickness in human knees, 1.75–2.75 mm [10,20,30], and more representative of human shoulder cartilage thickness, $\sim$1.5 mm [13,34]. The thin bovine cartilage was evaluated in pilot scans, and a slice thickness of 0.7 mm was used in the current study. The current slice thickness is thinner than a previous MR study of human humeral/glenoid fossa cartilages, whose investigators used a 1.0 mm slice thickness and emphasized the need to acquire thin image slices when evaluating thin cartilages [13].

The specimen was also submerged in vegetable oil during scanning to aid in delineation of the articular surface. Previous investigators noted difficulty in defining the articular surface in vivo due to opposing articulations, e.g., the load bearing region of the femoral-tibial joint [10], as well as the presence of noise in MR images [11]. Volume averaging, related to voxel dimensions, also play a role in accurately defining articular layers [11]. We sought to maximize the accuracy of our thickness measurements by reducing these confounding factors. The signal from the vegetable oil was nulled in the fat-suppressed MR images, which facilitated definition of the articular surface. It is unlikely that submersion in oil altered the cartilage thickness, the paired measurements, and therefore the results, since indentation analysis was performed shortly after the MR scanning.

A primary difference between our study and previous studies was the focus on validating a cartilage thickness tool rather than validating cartilage volume measurements. Previous investigators calculated cartilage volume to evaluate OA over time [35], to assess risk factors associated with changes in cartilage volume [36], and to evaluate volume changes as a result of axial alignment of the skeleton [37]. Our primary interest in developing a tool for quantitative analysis of cartilage morphology was for localized cartilage thickness measurements. The studies listed above reported significant differences in cartilage volume; however, a change in bulk volume does not indicate the location of cartilage loss. We anticipate that our results will aid in validating a tool for clinical evaluation of in-vivo cartilage thickness. This tool could be used in the longitudinal assessment of regional thickness changes over time in OA cohorts and also in providing a digital template of the joint for the purposes of future tissue engineering efforts.

Acknowledgment

The authors would like to thank Mr. Vamsi Juluri and Dr. Tennyson Maliro for their assistance in performing these experiments. The authors also acknowledge the support of the Clark and Kirby Foundations and research support from General Electric Healthcare.

References

[1] Eckstein, F., Burstein, D., and Link, T. M., 2006, "Quantitative MRI of Cartilage and Bone: Degenerative Changes in Osteoarthritis," NMR Biomed., **19**(7), pp. 822–854.

[2] Centers for Disease Control and Prevention (CDC), 2001, "Prevalence of Disabilities and Associated Health Conditions Among Adults—United States, 1999," MMWR Morb Mortal Wkly Rep., **50**, pp. 120–125.

[3] Park, S., Krishnan, R., Nicoll, S. B., and Ateshian, G. A., 2003, "Cartilage Interstitial Fluid Load Support in Unconfined Compression," J. Biomech., **36**(12), pp. 1785–1796.
[4] Potter, H. G., Linklater, J. M., Allen, A. A., Hannafin, J. A., and Haas, S. B., 1998, "Magnetic Resonance Imaging of Articular Cartilage in the Knee. An Evaluation With Use of Fast-Spin-Echo Imaging," J. Bone Jt. Surg., Am. Vol., **80**(9), pp. 1276–1284.
[5] Mosher, T. J., and Dardzinski, B. J., 2004, "Cartilage MRI T2 Relaxation Time Mapping: Overview and Applications," Semin. Musculoskelet. Radiol., **08**(4), pp. 355–368.
[6] Li, X., Benjamin Ma, C., Link, T. M., Castillo, D. D., Blumenkrantz, G., Lozano, J., Carballido-Gamio, J., Ries, M., and Majumdar, S., 2007, "In Vivo T1ρ and T2 Mapping of Articular Cartilage in Osteoarthritis of the Knee Using 3T MRI," Osteoarthritis Cartilage, **15**(7), pp. 789–797.
[7] Kim, Y. J., Jaramillo, D., Millis, M. B., Gray, M. L., and Burstein, D., 2003, "Assessment of Early Osteoarthritis in Hip Dysplasia With Delayed Gadolinium-Enhanced Magnetic Resonance Imaging of Cartilage," J. Bone Jt. Surg., Am. Vol., **85-A**(10), pp. 1987–1992.
[8] Williams, A., Gillis, A., Mckenzie, C., Po, B., Sharma, L., Micheli, L., Mckeon, B., and Burstein, D., 2004, "Glycosaminoglycan Distribution in Cartilage as Determined by Delayed Gadolinium-Enhanced MRI of Cartilage (dGEMRIC): Potential Clinical Applications," AJR, Am. J. Roentgenol., **182**(1), pp. 167–172.
[9] Hunter, D. J., Le Graverand, M. P., and Eckstein, F., 2009, "Radiologic Markers of Osteoarthritis Progression," Curr. Opin. Rheumatol., **21**(2), pp. 110–117.
[10] Koo, S., Gold, G. E., and Andriacchi, T. P., 2005, "Considerations in Measuring Cartilage Thickness Using MRI: Factors Influencing Reproducibility and Accuracy," Osteoarthritis Cartilage, **13**(9), pp. 782–789.
[11] McGibbon, C. A., Bencardino, J., Yeh, E. D., and Palmer, W. E., 2003, "Accuracy of Cartilage and Subchondral Bone Spatial Thickness Distribution From MRI," J. Magn. Reson. Imaging, **17**(6), pp. 703–715.
[12] El-Khoury, G. Y., Alliman, K. J., Lundberg, H. J., Rudert, M. J., Brown, T. D., and Saltzman, C. L., 2004, "Cartilage Thickness in Cadaveric Ankles: Measurement With Double-Contrast Multi-Detector Row CT Arthrography Versus MR Imaging," Radiology, **233**(3), pp. 768–773.
[13] Graichen, H., Jakob, J., Von Eisenhart-Rothe, R., Englmeier, K. H., Reiser, M., and Eckstein, F., 2003, "Validation of Cartilage Volume and Thickness Measurements in the Human Shoulder With Quantitative Magnetic Resonance Imaging," Osteoarthritis Cartilage, **11**(7), pp. 475–482.
[14] Graichen, H., Von Eisenhart-Rothe, R., Vogl, T., Englmeier, K. H., and Eckstein, F., 2004, "Quantitative Assessment of Cartilage Status in Osteoarthritis by Quantitative Magnetic Resonance Imaging: Technical Validation for Use in Analysis of Cartilage Volume and Further Morphologic Parameters," Arthritis Rheum., **50**(3), pp. 811–816.
[15] Eckstein, F., Hudelmaier, M., Wirth, W., Kiefer, B., Jackson, R., Yu, J., Eaton, C. B., and Schneider, E., 2006, "Double Echo Steady State Magnetic Resonance Imaging of Knee Articular Cartilage at 3 Tesla: A Pilot Study for the Osteoarthritis Initiative," Ann. Rheum. Dis., **65**(4), pp. 433–441.
[16] Peterfy, C. G., Gold, G., Eckstein, F., Cicuttini, F., Dardzinski, B., and Stevens, R., 2006, "MRI Protocols for Whole-Organ Assessment of the Knee in Osteoarthritis," Osteoarthritis Cartilage, **14**, pp. 95–111.
[17] Cohen, Z. A., Mccarthy, D. M., Kwak, S. D., Legrand, P., Fogarasi, F., Ciaccio, E. J., and Ateshian, G. A., 1999, "Knee Cartilage Topography, Thickness, and Contact Areas From MRI: In-Vitro Calibration and In-Vivo Measurements," Osteoarthritis Cartilage, **7**(1), pp. 95–109.
[18] Eckstein, F., Gavazzeni, A., Sittek, H., Haubner, M., Losch, A., Milz, S., Englmeier, K. H., Schulte, E., Putz, R., and Reiser, M., 1996, "Determination of Knee Joint Cartilage Thickness Using Three-Dimensional Magnetic Resonance Chondro-Crassometry (3D MR-CCM)," Magn. Reson. Med., **36**(2), pp. 256–265.
[19] Kladny, B., Bail, H., Swoboda, B., Schiwy-Bochat, H., Beyer, W. F., and Weseloh, G., 1996, "Cartilage Thickness Measurement in Magnetic Resonance Imaging," Osteoarthritis Cartilage, **4**(3), pp. 181–186.
[20] Kladny, B., Martus, P., Schiwy-Bochat, K. H., Weseloh, G., and Swoboda, B., 1999, "Measurement of Cartilage Thickness in the Human Knee-Joint by Magnetic Resonance Imaging Using a Three-Dimensional Gradient-Echo Sequence," Int. Orthop., **23**(5), pp. 264–267.
[21] Karvonen, R. L., Negendank, W. G., Fraser, S. M., Mayes, M. D., An, T., and Fernandez-Madrid, F., 1990, "Articular Cartilage Defects of the Knee: Correlation Between Magnetic Resonance Imaging and Gross Pathology," Ann. Rheum. Dis., **49**(9), pp. 672–675.
[22] Muensterer, O. J., Eckstein, F., Hahn, D., and Putz, R., 1996, "Computer-Aided Three Dimensional Assessment of Knee-Joint Cartilage With Magnetic Resonance Imaging," Clin. Biomech. (Bristol, Avon), **11**(5), pp. 260–266.
[23] Yeh, L. R., Kwak, S., Kim, Y. S., Chou, D. S., Muhle, C., Skaf, A., Trudell, D., and Resnick, D., 1998, "Evaluation of Articular Cartilage Thickness of the Humeral Head and the Glenoid Fossa by MR Arthrography: Anatomic Correlation in Cadavers," Skeletal Radiol., **27**(9), pp. 500–504.
[24] Eckstein, F., Westhoff, J., Sittek, H., Maag, K. P., Haubner, M., Faber, S., Englmeier, K. H., and Reiser, M., 1998, "In Vivo Reproducibility of Three-Dimensional Cartilage Volume and Thickness Measurements With MR Imaging," AJR, Am. J. Roentgenol., **170**(3), pp. 593–597.
[25] Eckstein, F., Adam, C., Sittek, H., Becker, C., Milz, S., Schulte, E., Reiser, M., and Putz, R., 1997, "Non-Invasive Determination of Cartilage Thickness Throughout Joint Surfaces Using Magnetic Resonance Imaging," J. Biomech., **30**(3), pp. 285–289.
[26] Haubner, M., Eckstein, F., Schnier, M., Losch, A., Sittek, H., Becker, C., Kolem, H., Reiser, M., and Englmeier, K. H., 1997, "A Non-Invasive Technique for 3-Dimensional Assessment of Articular Cartilage Thickness Based on MRI. Part 2: Validation Using CT Arthrography," Magn. Reson. Imaging, **15**(7), pp. 805–813.
[27] Eckstein, F., Schnier, M., Haubner, M., Priebsch, J., Glaser, C., Englmeier, K. H., and Reiser, M., 1998, "Accuracy of Cartilage Volume and Thickness Measurements With Magnetic Resonance Imaging," Clin. Orthop. Relat. Res., **1**(352), pp. 137–148.
[28] Naredo, E., Acebes, C., Moller, I., Canillas, F., De Agustin, J. J., De Miguel, E., Filippucci, E., Iagnocco, A., Moragues, C., Tuneu, R., Uson, J., Garrido, J., Delgado-Baeza, E., and Saenz-Navarro, I., 2009, "Ultrasound Validity in the Measurement of Knee Cartilage Thickness," Ann. Rheum. Dis., **68**, pp. 1322–1327.
[29] Mathiesen, O., Konradsen, L., Torp-Pedersen, S., and Jorgensen, U., 2004, "Ultrasonography and Articular Cartilage Defects in the Knee: An In Vitro Evaluation of the Accuracy of Cartilage Thickness and Defect Size Assessment," Knee Surg. Sports Traumatol. Arthrosc, **12**(5), pp. 440–443.
[30] Bowers, M. E., Trinh, N., Tung, G. A., Crisco, J. J., Kimia, B. B., and Fleming, B. C., 2008, "Quantitative MR Imaging Using 'Livewire' to Measure Tibiofemoral Articular Cartilage Thickness," Osteoarthritis Cartilage, **16**(10), pp. 1167–1173.
[31] Shrivastava, N., Koff, M. F., Abbot, A. E., Mow, V. C., Rosenwasser, M. P., and Strauch, R. J., 2003, "Simulated Extension Osteotomy of the Thumb Metacarpal Reduces Carpometacarpal Joint Laxity in Lateral Pinch," J. Hand Surg. [Br], **28**(5), pp. 733–738.
[32] Bland, J. M., and Altman, D. G., 1986, "Statistical Methods for Assessing Agreement Between Two Methods of Clinical Measurement," Lancet, **1**(8476), pp. 307–310.
[33] Glüer, C.-C., Blake, G., Lu, Y., Blunt, B. A., Jergas, M., and Genant, H. K., 1995, "Accurate Assessment of Precision Errors: How to Measure the Reproducibility of Bone Densitometry Techniques," Osteoporosis Int., **5**(4), pp. 262–270.
[34] Soslowsky, L. J., Flatow, E. L., Bigliani, L. U., and Mow, V. C., 1992, "Articular Geometry of the Glenohumeral Joint," Clin. Orthop. Relat. Res., **285**, pp. 181–190.
[35] Raynauld, J. P., Martel-Pelletier, J., Berthiaume, M. J., Beaudoin, G., Choquette, D., Haraoui, B., Tannenbaum, H., Meyer, J. M., Beary, J. F., Cline, G. A., and Pelletier, J. P., 2006, "Long Term Evaluation of Disease Progression Through the Quantitative Magnetic Resonance Imaging of Symptomatic Knee Osteoarthritis Patients: Correlation With Clinical Symptoms and Radiographic Changes," Arthritis Res. Ther., **8**(1), p. R21.
[36] Ding, C., Martel-Pelletier, J., Pelletier, J. P., Abram, F., Raynauld, J. P., Cicuttini, F., and Jones, G., 2008, "Two-Year Prospective Longitudinal Study Exploring the Factors Associated With Change in Femoral Cartilage Volume in a Cohort Largely Without Knee Radiographic Osteoarthritis," Osteoarthritis Cartilage, **16**(4), pp. 443–449.
[37] Eckstein, F., Wirth, W., Hudelmaier, M., Stein, V., Lengfelder, V., Cahue, S., Marshall, M., Prasad, P., and Sharma, L., 2008, "Patterns of Femorotibial Cartilage Loss in Knees With Neutral, Varus, and Valgus Alignment," Arthritis Rheum., **59**(11), pp. 1563–1570.